Buckling and vibration behavior of a non-uniformly heated isotropic cylindrical panel

Vinod S. Bhagat[a], Jeyaraj Pitchaimani[*] and S.M. Murigendrappa[b]

Department of Mechanical Engineering, National Institute of Technology Karnataka, Surathkal, Mangalore, 575025, India

Abstract. This study attempts to address the buckling and free vibration characteristics of an isotropic cylindrical panel subjected to non-uniform temperature rise using numerical approach. Finite element analysis has been used in the present study. The approach involves three parts, in the first part non-uniform temperature field is obtained using heat transfer analysis, in the second part, the stress field is computed under the thermal load using static condition and, the last part, the buckling and pre-stressed modal analysis are carried out to compute critical buckling temperature as well as natural frequencies and associated mode shapes. In the present study, the effect of non-uniform temperature field, heat sink temperatures and in-plane boundary constraints are considered. The relation between buckling temperature under uniform and non-uniform temperature fields has been established. Results revealed that decrease (Case (ii)) type temperature variation field influences the fundamental buckling mode shape significantly. Further, it is observed that natural frequencies under free vibration state, decreases as temperature increases. However, the reduction is significantly higher for the lowest natural frequency. It is also found that, with an increase in temperature, nodal and anti-nodal positions of free vibration mode shapes is shifting towards the location where the intensity of the heat source is high and structural stiffness is low.

Keywords: cylindrical panel; buckling strength; free vibration frequencies; free vibration mode shapes; finite element method

1. Introduction

Cylindrical panel is a mainstay in many engineering structures such as nuclear reactor components, supersonic and hypersonic aircraft components and, special storage tanks, due to its high load-carrying capacity, high stiffness and containment of space (Al-Khaleefi 2004). Thermal buckling is a commonly observed failure mode in such panels when exposed to heat. The dynamic behavior of these heated panels is substantially different from the dynamic characteristics under free stress condition.

Many literatures (e.g., Chen and Chen 1987, Jeng-Shian and Wei-Chong 1991, Averill and

---

[*]Corresponding author, Assistant Professor, E-mail: pjeyaemkm@gmail.com
[a]Ph.D., E-mail: vinbha2011@gmail.com
[b]Associate Professor, E-mail: smm@nitk.ac.in

Reddy 1993) reports on thermal buckling of the curved shells under uniform thermal load with external boundary constraints. However, the thin cylindrical shell panels exposed to non-uniform temperature distributions are prone to thermal buckling. In certain cases, the non-uniform thermal load plays a significant role in deciding and controlling the part design. The free vibration behavior of the heated panel members are significantly influenced by the thermal stress developed due to the thermal load. Chen and Chen (1987) have studied buckling characteristics of laminated cylindrical panels exposed to a uniform change in temperature rise using Galerkin's method. They observed that the buckling strength is affected by fiber alignment, plate curvature, aspect ratio and boundary conditions. Jeng-Shian and Wei-Chong (1991) used higher order displacement functions based a finite element method, to analyze the buckling behavior of anti-symmetric angle-ply laminated cylindrical shells exposed to a uniform temperature rise. Response of laminated cylindrical panels exposed to uniform temperature distribution was investigated by Averill and Reddy (1993) using higher-order shear deformation theory. The buckling behavior of the thin circular cylindrical shell with clamped edge under uniform thermal load was studied by Ross *et al*. (1966) using experiments. Shear deformation theory of higher order was developed for laminated shells with orthotropic layers and Navier-type exact results for free vibration was presented by Reddy and Liu (1985) for spherical and cylindrical shell with simply supported boundary conditions. Baruta *et al*. (2000) studied the influence of non-uniform thermal load on the stability of flat and curved laminates using nonlinear finite element analysis. Thermal load assumed was varying both through the thickness and over the surface of the panels. The buckling behavior of laminated plate subjected to uniform and non-uniform temperature rise was studied by Chen *et al*. (1991) using finite element method. The free vibration analysis of laminated cylindrical shell was carried out by Narita *et al*. (1993) using finite element approach wherein the influence of cross ply stacking sequences and the composite material constants on the vibration behavior was investigated. The influence of natural frequencies of spherical shells was studied by Buchanan and Rich (2002) using a nine-node Lagrange finite element with three different boundary conditions namely free, simply supported and fixed. SK & Sinha (2005) have developed a finite element method of doubly multilayered curved composite shells using Koiters shell theory and Mindlin's hypotheses. Zhao *et al*. (2004) has examined cylindrical panels under different boundary conditions to analyze the frequency behavior. Mesh free kp-Ritz method was used to analyze the effects of curved-edge boundary conditions on the frequency behavior of cylindrical panels. The vibration behavior of laminated composite shells was studied by Kurpa *et al*. (2010) using *R*-function theory and variational methods based on shear deformation theory of first order.

A few literatures listed below reports on the free vibration behavior of metallic structures subjected to thermal load. Buckling and free vibration of cylindrical shells with functionally graded material was studied by Kadoli and Ganesan (2006) when they are exposed to a temperature-definite boundary condition using finite element method, based on shear deformation theory of first order. Ganapathi *et al*. (2002) investigated the dynamic behavior of laminated cross-ply composite non-circular thick cylindrical shells exposed to thermal/mechanical load based on the higher-order shear deformation theory. Finite element method in conjunction with the direct time integration technique has been used to obtain shell responses. Jeon and Lee (2010) studied the free vibration behavior of cylindrical shell subjected to thermal load. The study was done using finite element software (ABAQUS) and modal analysis was carried out by experimentally. Buckling and vibration characteristics of circular cylindrical shells carrying hot liquid were analyzed by Ganesan and Pradeep (2005) using semi analytical finite element method. Wherein free vibration study was done by inculcating mass effect and initial stress effect because of hot

liquid.

Based on the literature, in the present study, detailed investigation on combined buckling and free vibration behavior of non-uniformly heated cylindrical panel is not investigated by researchers which is very important in the practical point of view. A few literature reports on heated cylindrical panels were limited to uniform and temperature variation along with either one-dimension or through the thickness direction. In practice, most of the panels are subjected to arbitrarily varying non-uniform temperature fields due to both the un-symmetric geometric variation and nature of heat source.

2. Analysis approach

In the present study, thermal buckling and free vibration behavior of the cylindrical panel exposed to non-uniform temperature fields is investigated numerically. Initially, heat transfer analysis was carried out to compute temperature field associated with a particular temperature boundary condition. Then, a static structural analysis was carried out to account for thermal load as pre-stress state. Finally, first four natural frequencies associated with mode shapes were obtained at critical buckling temperature under pre-stress state. A commercially available finite element tool (ANSYS) has been used. The scheme of numerical analysis is as shown in Fig. 1.

2.1 Finite element formulation

2.1.1 Heat transfer analysis

Heat transfer analysis is used to obtain the temperature distribution across the surface of the cylindrical panel for various heat distribution. A two dimensional eight noded rectangular element is used to obtain the temperature distribution on the panel. The two dimensional steady state heat conduction equation without heat generation is

$$K\left(\frac{\partial^2 T}{\partial x_1^2} + \frac{\partial^2 T}{\partial x_2^2}\right) = 0 \tag{1}$$

where K is thermal conductivity and T is the temperature. The variational form of the above governing equation is

$$I = \frac{1}{2}\int_a \{\nabla T\}^T [K]\{\nabla T\} da + \frac{1}{2}\int_{S_1} hT^2 dS - \int_{S_1} hT_\infty dS - \int_{S_2} qT dS \tag{2}$$

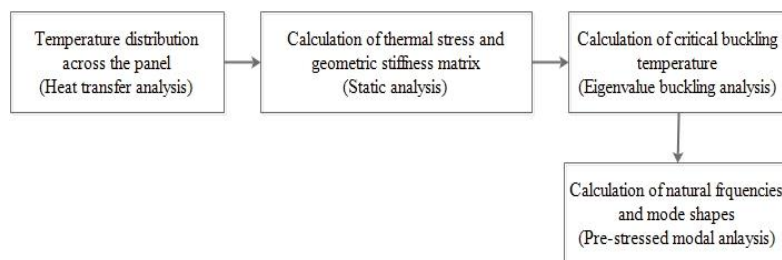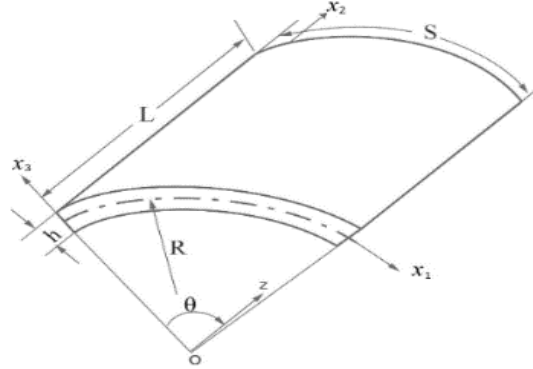Fig. 1 A scheme of numerical analysis

Fig. 2 Geometry of Cylindrical panel

where ∇T is temperature gradient vector. S_1 is convection heat transfer boundary. S_2 is the heat flux specified boundary, h is the convection heat transfer coefficient. T_∞ is the ambient temperature and q is the heat flux. Considering there is no internal heat generation and heat flow is mainly due to conduction mode. Following the finite element procedure and minimizing the above variational expression with respect to nodal temperature T_e, one can obtain.

$$[K_c]\{T_e\} = \{0\} \tag{3}$$

where conduction matrix is obtained by using Eq. (4).

$$[K_c] = K \iint [B_t]^T [B_t] dx_1 dx_2 \tag{4}$$

$[B_t]$ is the temperature gradient matrix, $[K_c]$ is the conduction matrix.
By solving Eq. (3), temperature variation across the cylindrical panel surface will be obtained according to the temperature boundary conditions specified along the edge of the panel.

2.1.2 Structural analysis

A cylindrical panel of width S, length L, thickness h and radius R measured from the mid depth of thickness is shown in Fig. 2. An orthogonal curvilinear coordinate system (x_1, x_2, x_3) is placed at $h/2$ and S and L are measured along the x_1 and x_2 axes, respectively. The surface generated by x_1-x_2 is the reference surface ($x_3=0$) and x_3 is normal to the x_1-x_2 surface. The following is the strain-displacement relations for cylindrical panels (Al-Khaleefi 2004)

$$\begin{Bmatrix} \varepsilon_x^0 \\ \varepsilon_y^0 \\ \varepsilon_{xy}^0 \end{Bmatrix} = \begin{Bmatrix} \dfrac{\partial u^0}{\partial x_1} + \dfrac{w^0}{R} \\ \dfrac{\partial v^0}{\partial x_2} \\ \dfrac{\partial u^0}{\partial x_2} + \dfrac{\partial v^0}{\partial x_1} \end{Bmatrix} \tag{5}$$

where ε_x^0 and ε_y^0 represent strain components at mid-plane ($x_3=0$), ε_{xy}^0 represent the in-plane shear strain. u^0, v^0, w^0 represents displacement of reference surface along x_1, x_2 and x_3

respectively. Strain at any point along the thickness is as given below

$$\begin{Bmatrix} \varepsilon_x \\ \varepsilon_y \\ \varepsilon_{xy} \end{Bmatrix} = \begin{Bmatrix} \varepsilon_x^0 \\ \varepsilon_y^0 \\ \varepsilon_{xy}^0 \end{Bmatrix} + x_3 \begin{Bmatrix} k_x \\ k_y \\ k_{xy} \end{Bmatrix} \qquad \therefore \{\varepsilon\} = \{\varepsilon^0\} + x_3\{k\} \tag{6}$$

where $\{\varepsilon\}$, $\{k\}$ are the in-plane linear strain vector and the curvature strain vector, respectively. The constitutive relations for an isotropic cylindrical panel considering thermal effects are as given below.

$$\begin{Bmatrix} \sigma_x \\ \sigma_y \\ \sigma_{xy} \end{Bmatrix} = E \begin{Bmatrix} \varepsilon_x^0 - \alpha\nabla T(x_1, x_2) \\ \varepsilon_y^0 - \alpha\nabla T(x_1, x_2) \\ \varepsilon_{xy}^0 - \alpha\nabla T(x_1, x_2) \end{Bmatrix} \qquad \therefore \{\sigma\} = E\{\varepsilon - \alpha\nabla T(x_1, x_2)\} \tag{7}$$

where E, α, $\Delta T(x_1, x_2)$ are Young's modulus, coefficient of thermal expansion and temperature difference function (temperature variation along the panel surface), respectively. Force and moment resultant vector due to change in temperature are given by

$$\begin{Bmatrix} N_x^T \\ N_y^T \\ N_{xy}^T \end{Bmatrix} = E\alpha \int_{-h/2}^{h/2} \nabla T(x_1, x_2) dx_3 \qquad ; \qquad \begin{Bmatrix} M_x^T \\ M_y^T \\ M_{xy}^T \end{Bmatrix} = E\alpha \int_{-h/2}^{h/2} \nabla T(x_1, x_2) x_3 dx_3 \tag{8}$$

By following the usual finite element procedure, structural stiffness matrix, geometric stiffness matrix and mass matrix can be obtained. Cylindrical shell panel is exposed to membrane compressive load due to the non-uniform temperature and structural boundary constraints which is calculated by using static analysis. Static analysis is carried out using structural stiffness matrix $[K]$, load vector due to change in temperature $\{F\}$ and nodal displacement vector $\{U\}$.

$$[K]\{U\} = \{F\} \tag{9}$$

The structural stiffness matrix is given by

$$[K] = \iint [B]^T [E][B] dx_1 dx_2 \tag{10}$$

where $[B]$ is the linear strain displacement matrix, which relates nodal displacement to the strain in the element. $[E]$ is the constitutive matrix which defines stress strain relation of the material. Similarly, the geometric stiffness matrix $[K_\sigma]$ is calculated from the work done by the membrane forces developed due to thermal load.

$$[K_\sigma] = \iint [G]^T [S][G] dx_1 dx_2 \tag{11}$$

$[G]$ obtained from shape function by appropriate differentiations. $[S]$ contains the initial stress terms obtained from static analysis.

$$[S] = \begin{bmatrix} S_x & S_{xy} \\ S_{xy} & S_y \end{bmatrix} \tag{12}$$

The membrane forces S_x, S_y and S_{xy} are specified in terms of membrane stresses σ_x, σ_y and shear stress σ_{xy} developed due to thermal load and are calculated from a static analysis.

Buckling analysis is carried out using the structural stiffness matrix $[K]$ and geometric stiffness matrices $[K_\sigma]$ based on the relation given in Eq. (13)

$$([K] + \lambda_i [K_\sigma])\{\psi_i\} = 0 \tag{13}$$

where, λ_i is the ith Eigen value and $\{\psi_i\}$ is the corresponding Eigen vector. The product of the temperature rise ΔT (above ambient temperature) and the lowest Eigen value λ_i gives the critical buckling temperature T_{cr} that is $T_{cr} = \lambda_1 \Delta T$. In the case of non-uniform temperature variation, ΔT is maximum temperature of a particular temperature profile. Since the panel is pre-stressed due to the thermal field, structural stiffness of the panel will change in turn it will change the natural frequencies of the panel. In order to find the effect of thermal stress on the natural frequencies and their corresponding mode shapes, pre-stressed modal analysis is carried out using Eq. (14).

$$(([K] + [K_\sigma]) - \omega_k^2 [M])\{\phi_k\} = 0 \tag{14}$$

To calculate the natural frequency and mode shape at a particular temperature above ambient temperature geometric stiffness matrix will be obtained at that temperature and will be given as input to Eq. (14). where, $[M]$ is the structural mass matrix, ω_k is the natural frequency of the pre-stressed structure, $\{\Phi_k\}$ the corresponding mode shape, while $[N]$ shape function matrix and $[\rho]$ inertia matrix is used to obtain the structural mass matrix given by Eq. (15)

$$[M] = \iint [N]^T [\rho][N] dx_1 dx_2 \tag{15}$$

Temperature distribution on the cylindrical panel subjected to non-uniform temperature field is determined using FEA tool. The panel is modelled using an eight node isoparametric thermal shell element (SHELL131). While performing heat transfer analysis, it is assumed that there is no temperature variation across the thickness of the panel i.e., x_3-direction. Nodal temperatures obtained from the heat transfer analysis are then imported in static analysis to compute thermal stress wherein an eight node isoparametric structural shell element (SHELL281) is used, followed by an eigenvalue buckling analysis to predict critical buckling temperature. Finally, pre-stressed modal analysis as a function of critical buckling temperature is carried out to analyze the influence on free vibration characteristics, such as natural frequencies and associated mode shapes.

3. Validation studies

3.1 Thermal buckling

The thermal buckling behavior of a fully clamped cylindrical panel examined by Al-Khaleefi (2004) has been considered for the validation. The dimensions of the panel are h=1 mm, S/h=40, R/S=10 and L/S=1 with following properties; Young's modulus (E)=40 GPa, Poisson's ratio (μ)=0.25, coefficient of thermal expansion (α)=79×10^{-6}/°C. Wherein Al-Khaleefi (2004) has used an analytical approach, based on the first-order shear deformation shell theory. Based on the present study the critical buckling temperature matches with that of Al-Khaleefi (2004).

Table 1 Comparison of natural frequencies (Hz) with Au and Cheung (1996)

Mode	Natural frequencies	
	Au and Cheung (1996)	Present study
1	869	869
2	957	957
3	1287	1287
4	1363	1363

3.2 Free vibration

The free vibration behavior of a fully clamped cylindrical panel investigated by Au and Cheung (1996) has been considered for the validation. Au and Cheung (1996) obtained natural frequencies of the cylindrical panel using isoparametric spline finite strip method, while the present method uses FEA tool. The panel is made of aluminum with the following mechanical properties; Young's modulus (E)=68.9 GPa, Poisson's ratio (μ)=0.33 and density (ρ)=2657 kg/m^3. The dimensions of the panel are θ=0.133 rad, h=0.33 mm, S=76.2 mm, L/S=1 and R=762 mm. The results obtained using present study matches well with that of results reported in Au and Cheung (1996). Table 1 presents the natural frequencies of the panel.

4. Results and discussion

Fig. 2 depicts the schematic diagram of cylindrical panel analyzed in the present study with a thickness (h), angle of curvature (θ), mean radius of curvature (R), length of the panel (L) and width of the panel (S). An orthogonal curvilinear coordinate system (x_1, x_2, x_3) is positioned at $h/2$. In-plane displacements denoted by u_0, v_0 and w_0 are considered in x_1, x_2 and x_3-directions, respectively. Similarly, θ_x and θ_y are the rotations in x_1 and x_2 directions, respectively.

A cylindrical panel of thickness (h)=1 mm, thickness ratio (S/h)=150, curvature ratio (R/S)=2 and angle of curvature (θ)=45° is considered in the investigation. Cylindrical panel is assumed to be made of mild steel with following properties; Young's modulus (E)=210 GPa, Poisson's ratio (μ)=0.3, coefficient of thermal expansion (α)=12.6×10^{-6}/^{o}C and density (ρ)=7850 kg/m^3. The investigation is carried out for two aspect ratios of the panel and three different structural boundary conditions. The first aspect ratio is L/S=1 denoted by panel-1 and the second aspect ratio is 1.5 denoted by panel-2. Whereas, the boundary conditions of type CCCC, CCFC and SSSS (where C-clamped, S-simply supported and F-free). The first letter in these boundary conditions is associated with forefront curved edge at x_2=0 in order as presented in Table 2. CCCC boundary conditions are utilized to simulate the panel constrained from all sides. Whereas, CCFC boundary conditions are used to investigate the effect of free edge on the buckling and the free vibration behavior of the panel. SSSS boundary conditions are utilized to study the effect of non-uniform temperature distribution on the buckling strength when free expansion is allowed along the in-plane direction. Material properties are assumed to be temperature independent. However, it is ensured that the temperature range analysed does not change the material properties significantly with temperature rise.

Table 2 Structural boundary constraints used for the analysis
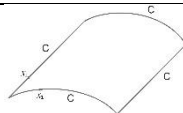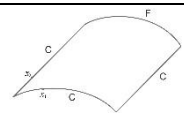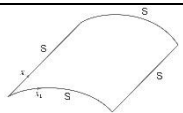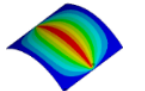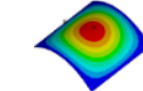
Structural boundary constraints		
CCCC	CCFC	SSSS
$x_1 = 0, S$ $u_0 = v_0 = w_0 = 0$ $\theta_x = \theta_y = 0$ $x_2 = 0, L$ $u_0 = v_0 = w_0 = 0$ $\theta_x = \theta_y = 0$	$x_1 = 0, S$ $u_0 = v_0 = w_0 = 0$ $\theta_x = \theta_y = 0$ $x_2 = 0$ $u_0 = v_0 = w_0 = 0$ $\theta_x = \theta_y = 0$	$x_1 = 0$ $u_0 = w_0 = 0$ $x_1 = S$ $w_0 = 0$ $x_2 = 0$ $v_0 = w_0 = 0$ $x_2 = L$ $w_0 = 0$

Table 3 Different temperature distribution field analyzed

	Temperature distribution cases				
Position of heat source	Case (i)	Case (ii)	Case (iii)	Case (iv)	Case (v)
	Uniform				
Thermal distribution					
Boundary constraints	$T=1\,°C$ at $x_1 = 0; x_1 = S$	$T=0\,°C$ at $x_1 = 0; x_1 = S$	$T=0\,°C$ at $x_1 = 0; x_1 = S$	$T=0\,°C$ at $x_1 = 0; x_1 = S$ $x_2 = 0; x_2 = L$	$T(x_1, x_2) =$ $\sin(\pi x_1/S) \sin(\pi x_2/L)$
	$T=1\,°C$ at $x_2 = 0; x_2 = L$	$T=1\,°C$ at $x_2 = 0$ $T=0\,°C$ at $x_2 = L$	$T=1\,°C$ at $x_2 = 0; x_2 = L$	$T=1\,°C$ at $x_2 = L/2$	

*Blue: ambient temperature; Red: 1°C above ambient temperature and others in-between

4.1 Non-uniform temperature distributions

Present study employs four different non-uniformly varying in-plane temperature distribution according to the nature of the assumed temperature source of a cylindrical panel and since the thickness of the cylindrical shell analyzed is very small, it is assumed that the temperature variation in the thickness direction is constant. Further, same non-uniform temperature distributions have been considered to investigate their effect on thermal buckling and free vibration characteristics of the cylindrical panel. Columns of heating furnace, electronic circuit board, nuclear vessels, and automobile panels located above engine, structures used in aerospace vehicles such as high-speed aircrafts and components of rockets and missiles are typical examples of structures exposed to non-uniform heating during their service. The uniform temperature field has also been considered for investigation, so that the change in buckling and free vibration behaviour of cylindrical panel with change in temperature field from uniform to non-uniform can be observed. The five cases of temperature variations are considered in the study; case (i)-uniform temperature field; case (ii)- decreasing trend in temperature field; case (iii)-decreasing and increasing trend in temperature field; case (iv)-increasing and decreasing trend in temperature field and case (v)-Camel hump trend in temperature field. Table 3 shows a cylindrical panel with the

position of the heat source, associated temperature fields and thermal boundary constraints. Initially highest temperature of a particular temperature variation is assumed 1°C above ambient temperature (other temperature values in between) in order to get the critical buckling temperature directly from the result of eigenvalue buckling analysis. However, the variation of natural frequencies and associated mode shapes are analyzed at different temperature level as a function critical buckling temperature.

4.2 Studies on cylindrical panel-1

4.2.1 Thermal buckling studies

The cylindrical panel is examined for two different dimension parameter ratio, namely the thickness ratio and curvature ratio along with five different temperature fields and three different structural boundary conditions in order to investigate buckling and free vibration characteristics of non-uniformly heated cylindrical panel. The relation between buckling temperature under uniform and non-uniform temperature field variation known as "Magnification factor of the first kind, η" proposed by Ko (2004) is evoked in the present study.

$$\eta = \frac{[T_o]_{cr}}{[T_c]_{cr}} \tag{16}$$

where $[T_o]_{cr}$ is the critical buckling temperature under non-uniform temperature field and $[T_o]_{cr}$ is critical buckling temperature under uniform temperature field. In this study peak temperature (T_o) of 1°C above ambient temperature is used and the heat sink temperature (T_s) is allowed to vary in the range of (T_s /T_o=0 to 1) and the relation is then established for different temperature cases. From this relation it is easy to get the critical buckling temperature of the panel under non-uniform temperature field, knowing the buckling temperature of the uniform temperature field. Table 4 shows the magnification factor of the first kind for different non-uniform temperature fields under CCCC boundary conditions. In Table 4, T_s /T_o=0 indicates that, the heat sink is at ambient temperature with a peak temperature of 1°C above ambient temperature in other words panel is subjected to non-uniform temperature field with higher temperature difference while T_s /T_o=1 indicates both heat-sink and peak temperature are at 1°C above ambient temperature which indicates that the panel is subjected to uniform temperature distribution field. From Table 4, it is clear that thermal buckling strength is significantly influenced by the nature of temperature variation as indicated by the values of the magnification factor of the first kind. It can be observed from Table 4 that the critical buckling temperature under case (i) temperature field has to be

Table 4 Magnification factor of the first kind for CCCC cylindrical panel-1

T_s/T_o	Case (ii)	η	Case (iii)	η	Case (iv)	η	Case (v)	η
0.0	431	2.60	247	1.49	383	2.31	279	1.68
0.2	333	2.01	226	1.36	304	1.83	248	1.49
0.4	268	1.61	208	1.25	252	1.52	221	1.33
0.6	224	1.35	192	1.16	215	1.30	200	1.20
0.8	191	1.15	178	1.07	189	1.14	182	1.10
1.0*	166	1.00	166	1.00	166	1.00	166	1.00

*Case (i) temperature field

Table 5 Magnification factor of the first kind for CCFC cylindrical panel-1

T_s/T_o	Case (ii)	η	Case (iii)	η	Case (iv)	η	Case (v)	η
0	514	2.12	411	1.69	560	2.30	482	1.98
0.2	426	1.75	368	1.51	460	1.89	421	1.73
0.4	361	1.49	330	1.36	384	1.58	366	1.51
0.6	312	1.28	296	1.22	325	1.34	318	1.31
0.8	273	1.12	268	1.10	279	1.15	277	1.14
1.0*	243	1.00	243	1.00	243	1.00	243	1.00

magnified by 2.6 to get the critical buckling temperature under case (ii) temperature field. Similarly, it has to be magnified by 1.49, 2.31 and 1.68 to get the critical buckling temperature of case (iii), case (iv) and case (v) respectively. Thermal buckling strength is found to be minimum when a major portion of the panel-1 is exposed to maximum temperature of the variation. From the study it has been found that, case (iii) and case (v) temperature field has the lowest magnification factor compared to others. Which indicates that more the panel surface is exposed to relatively higher temperatures in the variation, more the thermal stress will be developed and this will induce more membrane force in the panel, which inturn reduces the critical buckling temperature.

Panels with free edge, which allows in-plane free expansion when exposed to thermal load will behave differently from the panels without free edge, so CCFC cylindrical panel-1 is analyzed to investigate the effect of free edge on buckling behavior. Table 5 shows the magnification factor of the first kind of CCFC cylindrical panel-1. From Table 5, it is observed that, critical buckling strength of CCFC panel is also influenced by the nature of temperature variation. However, the variation of the buckling strength of the CCFC cylindrical panel-1 with the nature of temperature variation is not similar to the CCCC panel-1. Unlike the CCCC panel, buckling strength of CCFC panel is influenced by the level of temperature at the free edge for a particular temperature field. When the free edge is exposed to highest temperature of the variation, the panel-1 experiences lowest buckling strength as observed in the case (iv) in Table 5. It can be observed from Table 5 that buckling temperature under case (i) has to be magnified by 2.12, 1.69, 2.3 and 1.98 to get the buckling temperature under case (ii), case (iii), case (iv) and case (v) temperature field respectively. It can be clearly seen from Table 4 and Table 5 that CCCC cylindrical panel-1 has a lower critical buckling temperature compared to CCFC panel-1. This can be attributed to the free expansion due to heating associated with the CCFC panel-1 which allows some stress to relieve from the panel and thus produces less membrane force compared to CCCC panel-1.

In most of the real cases, the panel under thermal load tries to expand under heating, but its free expansion is prevented by the cooler boundary (heat sinks). This constraint due to non-uniform temperature will produce membrane compressive forces in the panel which results in thermal buckling. As the boundaries are heated up, constraints due to cooler boundaries will gradually relax, resulting in higher buckling temperature. In order to find out the influence of non-uniform temperature distribution field and heat sink temperature on the panel buckling temperature with free in-plane motion, a study has been carried out on a cylindrical panel-1 with simply supported boundary conditions with in-plane motions. The study will establish the "Magnification factor of the second kind, ξ" as proposed by Ko (2004) to relate the critical buckling temperature of a non-uniform temperature field obtained for an unheated boundary heat sink and for a boundary heat sink when heated up.

Table 6 Magnification factor of the second kind for SSSS cylindrical panel-1

T_s/T_o	Case (v)	ξ	Case (iv)	ξ
0	144	1.00	264	1.00
0.2	180	1.25	331	1.25
0.4	240	1.67	441	1.67
0.6	361	2.51	661	2.50
0.8	721	5.01	1323	5.01
1.0*	∞	∞	∞	∞

*Case (i) temperature field; **Exceeded melting range

$$\xi = \frac{\left[(T_o)_{cr}\right]_{(T_s \neq 0)}}{\left[(T_o)_{cr}\right]_{(T_s = 0)}} \tag{17}$$

where $[(T_o)_{cr}]_{(Ts \neq 0)}$ indicates the critical buckling temperature when heat sink temperature is not equal to zero whereas $[(T_o)_{cr}]_{(Ts = 0)}$ indicates the critical buckling temperature when heat sink temperature is zero. Simply supported cylindrical panel-1 with free in-plane motion is considered for the analysis along with two temperature distribution cases (case (iv) and case (v)), as in both the cases heat source is fully surrounded by cooler boundaries, hence the buckling behavior due to non-uniform temperature can be studied. Table 6 shows the magnification factor of second kind for SSSS cylindrical panel-1. It can be clearly observed from Table 6 that, case (v) has a lower buckling strength compared to the case (iv) due to the fact that, in the former the heat is applied in the region where the panel is less stiff. Results from the analysis mentioned in Table 6 indicates that buckling temperature increases with heat sink temperature and becomes infinity when temperature distribution is uniform throughout the panel. The panel experiences uniform temperature rise above ambient temperature when T_s equals to T_o. SSSS panel-1 analyzed allows free in-plane expansion and for the uniform temperature rise, the panel-1 does not experience any membrane compressive forces required for buckling. When the temperature distribution becomes non uniform, thermal stresses will be generated which will set up the required membrane force in the panel.

   To analyze the effect of different dimensional parameter on the critical buckling temperature, a cylindrical panel-1 with four different thickness ratio and curvature ratio has been considered. Fig. 3 indicates the influence of thickness ratio and nature of temperature field on the buckling strength of the panel-1 under CCCC and CCFC boundary conditions. Whereas Fig. 4 indicates the effect of curvature ratio and nature of temperature field on the thermal buckling strength of the cylindrical panel-1 under CCCC and CCFC boundary conditions. From Figs. 3-4 it can be noticed that both thickness ratio and curvature ratio is inversely proportional to the buckling temperature. As the thickness ratio and curvature ratio increases, the stiffness of the panel-1 decreases, which decreases the buckling strength of the panel-1. Similarly, it can also be observed from the results that the resistance to the thermal buckling decreases with the increases in curvature ratio and it attains the minimum value when the curvature ratio tends to infinity. This is due to the fact that moment of inertia decreases with increase in curvature ratio which reduces the bending stiffness of the panel and hence the buckling strength of the panel. Similar behavior can be noticed for all types of temperature variation field. One can observe that under CCCC boundary condition, case (ii) has the highest buckling temperature while for CCFC boundary conditions, case (iv) has

(a) CCCC panel   (b) CCFC panel
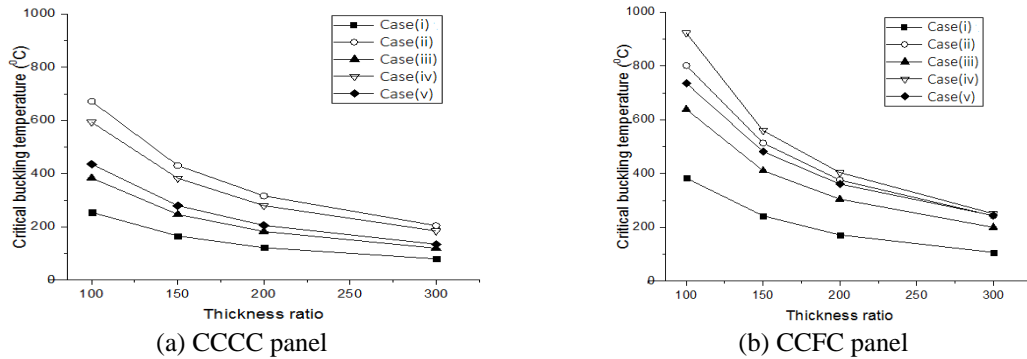
Fig. 3 Influence of thickness ratio and temperature variation on buckling strength of cylindrical panel-1

(a) CCCC panel   (b) CCFC panel
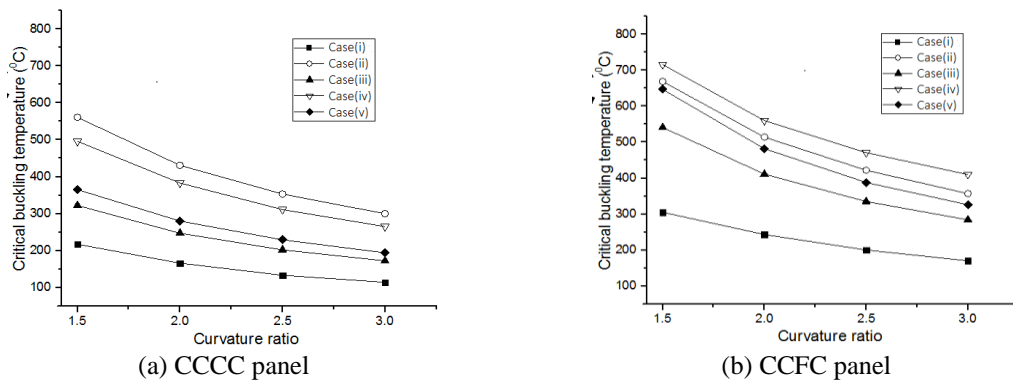
Fig. 4 Influence of curvature ratio and temperature variation on buckling strength of cylindrical panel-1

the highest buckling temperature. Whereas case (i) has a lowest buckling strength under both CCCC and CCFC boundary condition. Data obtained from Figs. 3-4 shows that, under CCCC boundary condition, case (ii) has the highest buckling temperature due to the fact that the heat source is found to be very close to clamped supports and the membrane compressive forces generated due to heat is balanced by support reaction forces, hence more heat is required to produce sufficient membrane compressive forces in-order to overcome the reaction forces and to cause buckling. Similarly, for the CCCC panel-1 exposed to case (iv) has a lower buckling strength than case (ii) mainly because the heat source is located away from the supports where the reaction forces are less and the panel is less stiff. Furthermore, the CCCC panel-1 under case (v) temperature variation field has a lower buckling strength compared to case (iv) due to the location of the heat source. Compared to other temperature variation fields discussed above case (iii) has lower buckling strength as it gets heat from two sides which produces more membrane compressive forces. Whereas the case (i) has a lowest buckling temperature compared to all cases, as the entire cylindrical panel is exposed to heat. Under CCFC boundary conditions, all the temperature field was found to have higher buckling strength compared to respective temperature field with CCCC boundary conditions. There is a small variation in the buckling strength order has been observed in CCFC boundary conditions compared to CCCC boundary conditions. In case of CCFC boundary conditions case (iv) has highest buckling temperature compared to other temperature fields due to the fact that the heat source is located close to free edge, thus some of the

thermal stress will be relieved from free edge which will produce a less membrane force.

Bending amplitude of the fundamental buckling mode associated with the center line of the cylindrical panel-1 along the longitudinal direction (x_2 - axis) is obtained to analyze the influence of temperature variation on the buckling mode shape. Fig. 5(a) shows influence of nature of temperature variation on buckling mode shape of CCCC panel-1. A panel with a thickness ratio of 150 and a curvature ratio of 2 with a thickness of 1mm has been considered for the investigation. From Fig. 5(a), one can observe that, the influence of temperature field on the buckling mode shape and its amplitude is significant. For the CCCC panel-1 exposed to case (ii) temperature field bending amplitude of the buckling mode has peak towards the heat source location and its response decreases for the peaks away from the heat source. Similarly, the CCCC panel-1 under case (i), bending amplitude of the buckling mode remains constant for all peaks due to the fact that the total area is exposed to constant thermal load. When the CCCC panel-1 exposed to temperature variation, the maximum amplitude of the buckling mode under case (iii) and case (v) is found to be at the center of the panel where the area is less stiff and for case (iv) there is not much variation in the amplitude of the peaks. It has also been noticed that for all temperature fields except case (ii) the behavior of peaks is symmetric about the central line of the panel. This can be attributed to the un-symmetric temperature variation associated with the case (ii) temperature field. Fig. 5(b) shows the non-dimensional bending amplitude associated with the buckling mode shape of CCFC panel-1. Compared to the CCCC panel-1, influence of nature of temperature variation on buckling mode shape of CCFC panel-1 is significant as seen in Fig. 5(b). In CCFC boundary conditions all temperature fields (case (i) to case (v)) have their highest amplitude peak away from the free edge. It is also observed that the amplitude of the peaks is dying out in the region close to free edge as it allows thermal stress to relieve from the free edge. Under CCFC boundary conditions case (iii) has the highest bending amplitude compared to others. The buckling mode shape pattern observed in CCFC panel-1 with case (ii) field follows the same trend as observed in CCCC boundary conditions with slight variation in amplitude due to the fact that the effect of free edge on panel with case (ii) temperature field is minimum as the heat source is far away from the free edge. Whereas for other cases the trend is changing significantly with modes moving towards the clamped edge due to un-symmetric boundary conditions. It can also be noted from Fig. 5(b) that maximum amplitude always occurs near edge opposite to the free edge this is due to the fact that at free edge there won't be any reaction forces which opposes the membrane forces, but at clamped edge there will be reaction forces which induces stress in the panel and thus making it to buckle.

(a) CCCC panel   (b) CCFC panel
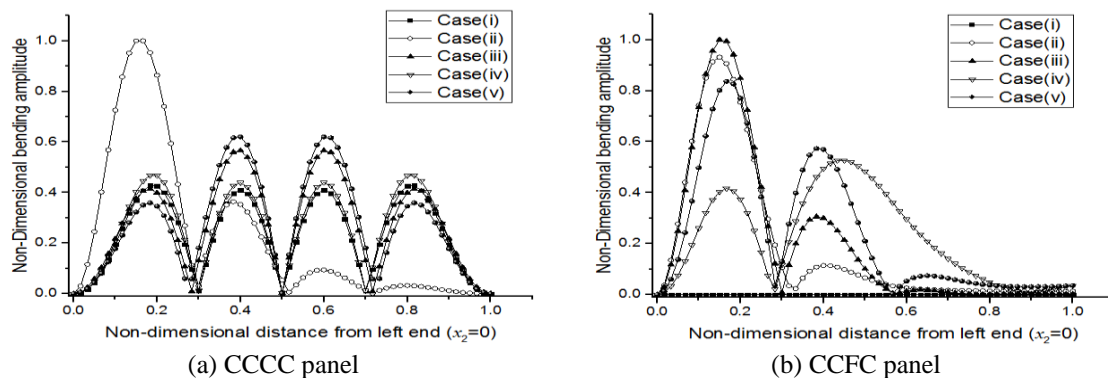
Fig. 5 Influence of nature of temperature variation on buckling mode shape of cylindrical panel-1

Table 7 Effect of thickness ratio on buckling mode shape of CCCC panel-1
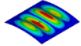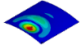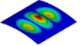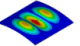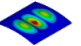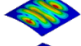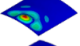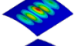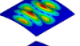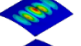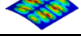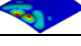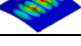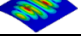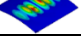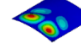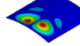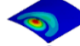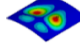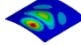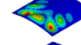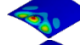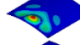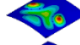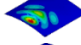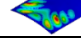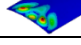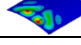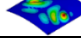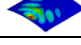
S/h	Case (i)	Case (ii)	Case (iii)	Case (iv)	Case (v)
100					
200					
300					

Table 8 Effect of thickness ratio on buckling mode shape of CCFC panel-1

S/h	Case (i)	Case (ii)	Case (iii)	Case (iv)	Case (v)
100					
200					
300					

Note: Dark-red: max.; dark-blue: min. and others-inbetween

Influence of thickness ratio and temperature field on the buckling mode shape of the CCCC and CCFC panels are shown in Tables 7-8 respectively. It can be clearly seen from Tables 7-8 that thickness ratio has a significant effect on the buckling mode shape as stiffness changes with the thickness ratio and similar behavior can be noticed for all the temperature field. From Table 7 one can observe that, the CCCC panel-1 under case(ii) temperature variation has buckling mode shapes with maximum bending amplitude towards the edge exposed to highest temperature of case (ii) field. While the edge opposite to this experience least bending amplitude. When the CCCC panel-1 is exposed to case (iii), case (iv) and case (v) temperature fields, there is no significant variation in buckling mode shapes while modal indices of the buckling mode shapes along the longitudinal (x_2) direction increases with the thickness ratio. When the CCCC panel-1 exposed to case (i) temperature field, modal indices along the longitudinal (x_2) direction increases with thickness ratio as seen for case (iii), case (iv) and case (v). However, when the thickness ratio is 300, buckling mode shape has modal indices of two along circumferential (x_1) direction. It can be observed from Table 8 that CCFC panel-1 under case (iv) temperature variation field has buckling mode shape with maximum bending amplitude at the mid portion which is exposed to highest temperature while the free edge experience least bending amplitude. Whereas for other cases, mode shape with maximum bending amplitude is found to occur away from free edge. It is important to know that, under all temperature variation cases bending amplitude of buckling mode shape is found to be minimum at the free edge.

Effect of curvature ratio and temperature variation on the buckling mode shape of CCCC and CCFC cylindrical panel-1 are shown in Table 9-10 respectively. Influence of curvature ratio on the buckling mode shape is significant due to change in moment of inertia with the curvature ratio.

As the curvature ratio increases, the maximum bending amplitude of the buckling mode of the CCCC panel-1 is moving towards the center of the panel where the panel is less stiff being case (ii) as exceptional. Table 10 depicts that, CCFC panel-1 under all temperature cases except case (iv) has maximum bending amplitude of buckling mode shape at the fixed edge opposite to free edge. For case (iv) temperature variation, the maximum bending amplitude of buckling mode occurs at central portion of the panel-1 which is subjected to maximum heat. It can also be noted

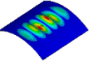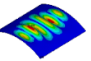Table 9 Effect of curvature ratio on buckling mode shape of CCCC panel-1
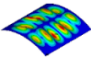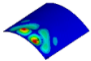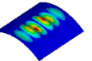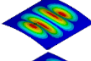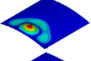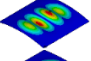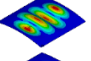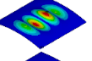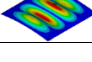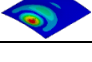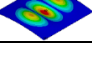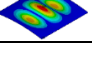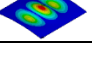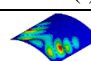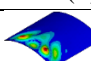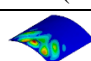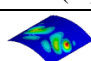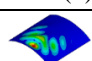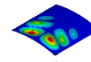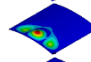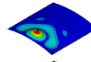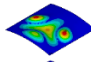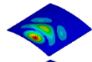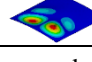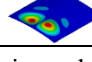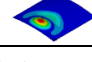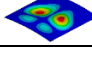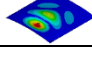
R/S	Case (i)	Case (ii)	Case (iii)	Case (iv)	Case (v)
1					
2					
3					

Table 10 Effect of curvature ratio on buckling mode shape of CCFC panel-1

R/S	Case (i)	Case (ii)	Case (iii)	Case (iv)	Case (v)
1					
2					
3					

Note: Dark-red: max.; dark-blue: min. and others-inbetween

Table 11 Effect of non-uniform thermal field on free vibration frequencies (Hz)

Mode	Ambient temperature	T_s/T_o (Case (v))						T_s/T_o (Case (iv))					
		0	0.2	0.4	0.6	0.8	1*	0	0.2	0.4	0.6	0.8	1*
1	177	130	146	157	165	171	177	156	161	165	169	173	177
2	210	192	196	200	204	207	210	196	199	202	205	207	210
3	303	292	297	299	301	302	303	288	292	295	298	301	303
4	334	307	313	320	325	330	334	321	324	327	329	331	334

*Case(i) temperature field

that as the curvature ratio increases modal indices of buckling modes along the longitudinal (x_2) direction decreases.

4.2.2 Free vibration studies

Pre-stressed modal analyses have been carried out on a cylindrical panel-1, to understand the behavior of free vibration and its mode shapes subjected to various temperature fields under different boundary conditions. To analyze the effect of heat sink temperature and non-uniform temperature field on the behavior of natural frequencies, a cylindrical panel exposed to two different temperature variation fields (case (iv) and case (v)) under simply supported boundary condition which allows in-plane motion is considered. Table 11 shows the effect of non-uniform temperature on free vibration frequencies of the simply supported cylindrical panel-1 with free in-plane motion. For the analysis, cylindrical panel subjected to a non-uniform temperature field with a peak temperature (T_o) of 100℃ above ambient temperature is considered and the heat sink temperature (T_s) is allowed to vary over the range of 0℃ to 100℃ above ambient temperature in the steps of 20℃ with no external in-plane boundary constraints. From Table 11, it is clear that free vibration frequency is minimum when the sink temperature is at 0℃ above ambient temperature and it increases with increase in sink temperature and becomes maximum when sink

Table 12 Effect of thermal load on free vibration frequency (Hz)

Boundary condition	Mode	Ambient Temp.	Case (i)		Case (ii)		Case (iii)		Case (iv)		Case (v)	
			$0.5*T_{cr}$	$0.95*T_{cr}$	$0.5*T_{cr}$	$0.95*T_{cr}$	$0.5*T_{cr}$	$0.95*T_{cr}$	$0.5*T_{cr}$	$0.95*T_{cr}$	$0.5*T_{cr}$	$0.95*T_{cr}$
CCCC	1	1359	1206	793	1246	738	1234	812	1191	801	1224	789
	2	1479	1331	851	1370	825	1359	922	1298	847	1339	862
	3	2071	1640	916	1713	1117	1681	1107	1695	865	1683	1080
	4	2075	1659	945	1732	1236	1706	1213	1697	979	1719	1182
CCFC	1	894	836	749	857	733	837	734	838	654	841	748
	2	1253	1203	754	1223	777	1187	751	1200	713	1199	772
	3	1597	1432	771	1459	823	1429	858	1420	1005	1408	960
	4	1615	1441	1059	1472	1175	1433	986	1421	1092	1413	1083

temperature equals to peak temperature in other words, when non-uniform temperature field becomes uniform. It is due to the fact that in the absence of external boundary constraints the panel under uniform temperature expands freely, hence does not produce any stress in the panel, whereas under non-uniform temperature field difference in peak temperature and sink temperature act as boundary constraints thus resist free expansion of the panel. Presence of thermal stress in the panel due to non-uniform temperature reduces the stiffness of the panel hence reduces the free vibration frequency.

To study the effect of thermal load on natural frequencies, cylindrical panel-1 exposed to the different temperature fields under clamped boundary conditions is considered, with critical buckling temperature as a one of the parameter. Table 12 shows the effect of thermal load on free vibration behavior of cylindrical panel-1 under CCCC boundary conditions. It has been noticed that free vibration frequency under ambient temperature reduces with increase in temperature under different temperature variation fields. Thermal load plays a major role in reducing the free vibration frequency of the heated cylindrical CCCC panel as it induces thermal stress in the panel, which inturn decreases the stiffness of the panel and stiffness is directly proportional to the frequency.

To analyze the combined effect of free edge and thermal load on the free vibration frequency, CCFC boundary conditions has been considered. There is not much variation can be noticed in the free vibration behavior of a CCFC cylindrical panel-1 subjected to different thermal load, as it allows some stress to relieve from the free edge. Mode shape also plays an important role while designing a thin structure of cylindrical panels as it gives the nodal and anti-nodal position of the particular mode through which mode can be excited. Hence it is very important to know the mode shape variation under thermal load along with the frequency.

From Table 13, it is clear that free vibration mode shapes changes very well with increase in temperature for all the temperature fields. Moving of nodal and anti-nodal positions and shifting of modes are commonly observed for the different temperature fields. For example, mode 1 of CCFC panel-1 having modal indices of (1,2) at ambient temperature changes to (1,3) at 95% of the critical buckling temperature under case (ii) temperature field as seen in Table 13. A similar trend has been observed for other vibration modes also. From Table 13 it can also be observed that for CCFC panel anti-nodal position of modes is moving towards the clamped edge with increase in temperature. For example, under case (iii) temperature field at ambient temperature, free vibration modes under mode 1 and mode 3 is found to occur at free edge, but with the increase in

Table 13 Effect of thermal load on the free vibration mode shape of panel-1

Temp. Variation cases	Temp.	CCFC					CCCC				
		Mode					Mode				
		1	2	3	4	5	1	2	3	4	5
	Ambient Temp.										
Case (i)	$0.5*T_{cr}$										
	$0.95*T_{cr}$										
Case (ii)	$0.5*T_{cr}$										
	$0.95*T_{cr}$										
Case (iii)	$0.5*T_{cr}$										
	$0.95*T_{cr}$										
Case (iv)	$0.5*T_{cr}$										
	$0.95*T_{cr}$										
Case (v)	$0.5*T_{cr}$										
	$0.95*T_{cr}$										

Note: Dark-red: max.; dark-blue: min. and others-inbetween

Table 14 Magnification factor of the first kind for CCCC cylindrical panel-2

T_s/T_o	Case (ii)	η	Case (iii)	η	Case (iv)	η	Case (v)	η
0	451	2.77	345	2.12	421	2.58	265	1.63
0.2	344	2.11	283	1.74	321	1.97	238	1.46
0.4	274	1.68	240	1.47	259	1.59	215	1.32
0.6	226	1.39	208	1.28	217	1.33	195	1.20
0.8	191	1.17	183	1.12	186	1.14	178	1.09
1.0*	163	1.00	163	1.00	163	1.00	163	1.00

temperature it is found to occur at fixed edge. This is due to the fact that with the increases in temperature, panel-1 becomes soft at the free edge, thus making the vibration modes to shift towards the stiffer side of the panel-1. The Influence of nature, of temperature variation on free vibration modes of the CCCC cylindrical panel-1 is also shown in Table 13. Compared to CCFC panel-1, variation of free vibration mode shapes of CCCC panel-1 with temperature variation is less. This can be attributed to the symmetric structural boundary and aspect ratio associated with the CCCC cylindrical panel-1. For CCCC panel under case (ii), modal indices changes from (1,2)

Table 15 Magnification factor of first the kind for CCFC cylindrical panel-2

T_s/T_o	Case (ii)	η	Case (iii)	η	Case (iv)	η	Case (v)	η
0	464	2.36	409	2.08	511	2.59	339	1.72
0.2	369	1.87	339	1.72	397	2.02	305	1.55
0.4	304	1.54	288	1.46	321	1.63	273	1.39
0.6	258	1.31	250	1.27	267	1.36	245	1.24
0.8	2 3	1.13	220	1.12	227	1.15	219	1.11
1.0*	197	1.00	197	1.00	197	1.00	197	1.00

*Case (i) temperature field

to (1,3) whereas for other cases it changes to (4,1) which shows that temperature has a significant effect on vibration mode shapes.

4.3 Studies on cylindrical panel-2

To know the effect of aspect ratio on the buckling and the free vibration behavior of a panel subjected to different temperature variation, a cylindrical panel-2 is considered for the investigation by keeping other dimensions same.

4.3.1 Thermal buckling studies

A cylindrical panel-2 is investigated for different parameters similar to the panel-1. Table 14 shows, magnification factor of the first kind obtained for fully clamped cylindrical panel-2. One can observe from Table 14 that magnification factor variation of a CCCC panel-2 is similar to the CCCC panel-1. Wherein the critical buckling temperature of CCCC panel-2 under case (i) has to be magnified by 2.77, 2.12, 2.58 and 1.63 to get the buckling solution of case (ii), case (iii), case (iv) and case (v) respectively. Table 14 also reveals that thermal buckling strength is directly proportional to the amount of region that the panel is exposed to maximum temperature under a particular temperature field and bending stiffness of that region. So compared to a cylindrical panel-1, cylindrical panel-2 has less stiffness, but it requires more heat to develop thermal stresses which can be noticed from the behavior of the panel-2 given in Table 14. Magnification factor of the first kind for a CCFC panel-2 is shown in Table 15. Data from Table 15 shows that, buckling temperature under case (i) temperature field has to be magnified by 2.36, 2.08, 2.59 and 1.72 to get the buckling solution of panel-2 under case (ii), case (iii), case (iv) and case (v) respectively. Analyses also shows that case (iv) temperature field has highest magnification factor under CCFC boundary condition but, not so for CCCC boundary condition. It is due to the fact that incase of case (iv) heat source is at the center of the panel, hence closer to the free edge therefore some of the stress set up due to thermal load will be relieved from the free edge.

To analyze the influence of heat sink temperature on the buckling strength in the absence of in-plane boundary constraints, a cylindrical panel-2 subjected to two different temperature fields under simply supported boundary conditions has been considered. Table 16 shows the magnification factor of second kind for a cylindrical panel-2 under simply supported boundary conditions with free in-plane motion. It is clear from Table 16 that, behavior of panel-2 is similar to panel-1 wherein buckling strength decreases with thermal stress set up due to non-uniform temperature. The buckling strength of cylindrical panel-2 is more than the cylindrical panel-1 when subjected to non-uniform temperature. Both cylindrical panel-2 and panel-1 used in the

Table 16 Magnification factor of the second kind for SSSS cylindrical panel-2

T_s/T_o	Case (v)	ξ	Case (iv)	ξ
0	213	1.00	333	1.00
0.2	266	1.25	416	1.25
0.4	355	1.67	555	1.67
0.6	532	2.50	832	2.50
0.8	1065	5.00	1666**	5.00
1.0*	∞	∞	∞	∞

*Case(i) temperature field; **Exceeded melting range

(a) CCCC panel   (b) CCFC panel
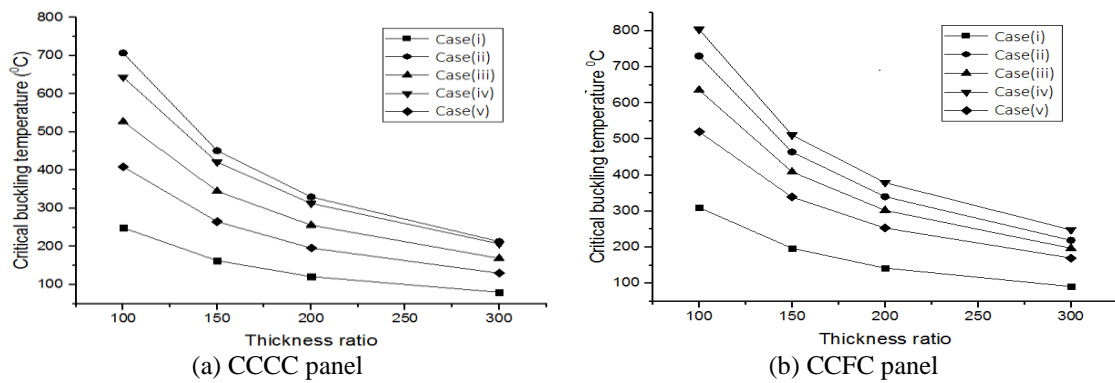
Fig. 6 Influence of thickness ratio and temperature variation on buckling strength of cylindrical panel-2

analysis has same width, from which the heat is supplied but since the length of the cylindrical panel-2 is more than the cylindrical panel-1, cylindrical panel-2 develops less membrane compressive force compared to cylindrical panel-1.

Dimension parameter study has also been carried out on a cylindrical panel-2 to know the effect of thickness ratio and curvature ratio on the critical buckling temperature. Fig. 6 shows the effect of thickness ratio and temperature variation on the buckling temperature of panel-2 under CCCC and CCFC boundary condition. It can be seen from Figs. 3a and 6a that buckling strength of the CCCC panel-2 under case (ii), case (iii) and case (iv) temperature variations is higher than the CCCC panel-1 under corresponding temperature variation. Whereas for case (i) and case (v) temperature field, the panel-2 has lower buckling strength compared to panel-1 as the structural stiffness of panel-2 is lesser than the panel-1 and under case (v) heat is supplied to the region which is having very less stiffness thus making it to buckle at low temperature. Even for the panel-2 buckling strength of the panel decreases with the increase in thickness ratio. It can be noted from Figs. 3(b) and 6(b) that the buckling strength of a CCFC panel-1 is higher than the CCFC panel-2 under all temperature fields due to fact that panel-1 has a higher stiffness than panel-2. Variation in the buckling strength under different temperature field decreases with the thickness ratio for the CCFC cylindrical panel-2 as seen Fig. 6(b).

Curvature ratio also plays an important role in deciding critical buckling temperature. Effect of curvature ratio on the buckling strength of the CCCC and CCFC panel-2 is shown in Fig. 7(a)-7(b) respectively. Where it can be seen that, as the curvature ratio increases the critical buckling temperature decreases. This behavior has been observed for all temperature field as the moment of

(a) CCCC panel   (b) CCFC panel
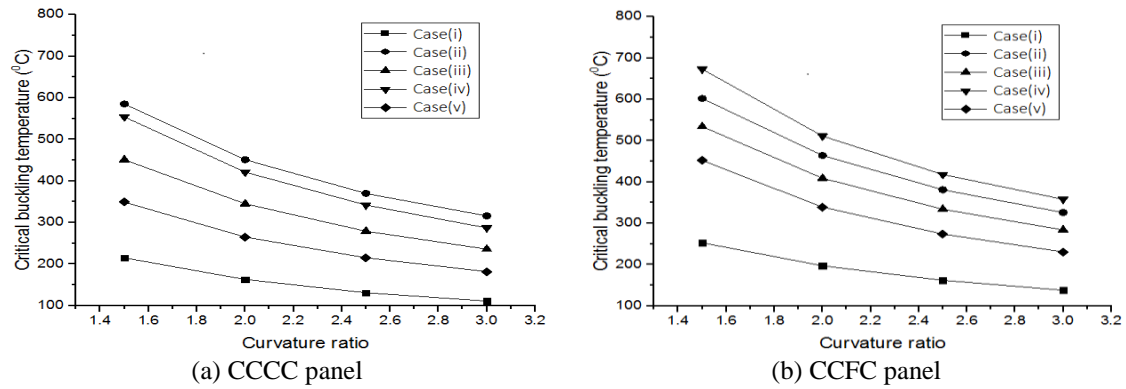
Fig. 7 Influence of curvature ratio and temperature variation on buckling strength of cylindrical panel-2

(a) CCCC panel   (b) CCFC panel
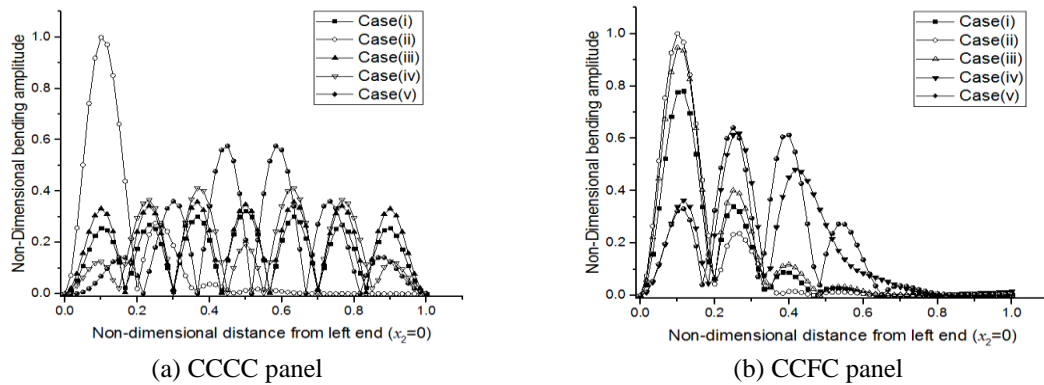
Fig. 8 Influence of nature of temperature variation on buckling mode shape of cylindrical panel-2

inertia plays dominating role in deciding the buckling strength of the panel.

Results obtained from Figs. 6-7 shows that, under CCCC boundary condition panel-2 behaves similar to the panel-1 under different temperature field. Wherein panel-2 under case (ii) temperature field has the highest buckling temperature and will have the lowest buckling strength under case (i). It also shows that case (iv), case (iii) and case (v) has lower buckling temperature compared to case (ii). Compare to other non-uniform temperature field case (v) has a significant effect on the buckling strength of the panel, as in case (v) the heat is applied in a region where there is less stiffness. Hence, one can notice that the buckling strength depends on the location of the heat source and amount of heat supplied to the panel. It has also been observed that, panel-2 under CCCC boundary conditions, was found to have lower buckling strength compared to panel-2 under CCFC boundary condition when subjected to different temperature fields. In case of CCFC boundary conditions case (iv) has highest buckling temperature compared to other temperature fields.

To analyze the influence of temperature variation on the buckling mode shape of panel-2, displacement associated with the center line of the cylindrical panel-2 along the longitudinal direction of the temperature variation is considered. Fig. 8(a) shows the non-dimensional bending amplitude associated with the fundamental buckling mode of the CCCC panel-2. Buckling mode shape for a panel-2 follows the same trend as observed for a panel-1. Even in panel-2 bending

Table 17 Effect of thickness ratio on buckling mode shape of CCCC panel-2
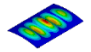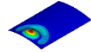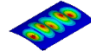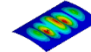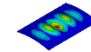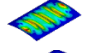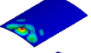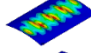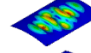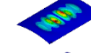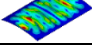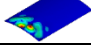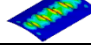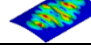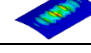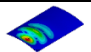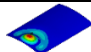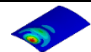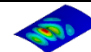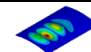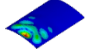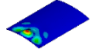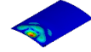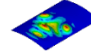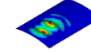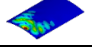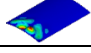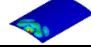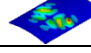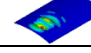
S/h	Case (i)	Case (ii)	Case (iii)	Case (iv)	Case (v)
100					
200					
300					

Table 18 Effect of thickness ratio on buckling mode shape of CCFC panel-2

S/h	Case (i)	Case (ii)	Case (iii)	Case (iv)	Case (v)
100					
200					
300					

Note: Dark-red: max.; dark-blue: min. and others-inbetween

amplitude for a case (ii) temperature field is high for a peak close to the heat source and its response decreases for the peaks away from the heat source. It can be seen from Fig. 8(a) that for case (i) and case (iv) temperature field, there is not much variation in the bending amplitude of the peaks. Whereas for case (iii) and case (v), peaks with high bending amplitude is found to be at the center of the panel. Fig. 8(b) shows the influence of nature, of temperature variation on the fundamental buckling modes of CCFC panel. In CCFC boundary conditions peaks with high amplitude is found to be located at the clamped edge under all temperature fields (case (i) to case (v)).

 In panel-2 under CCFC boundary conditions, case (ii) has the highest bending amplitude compared to others. The buckling mode shape pattern observed in CCFC panel-2 with case (ii) follows the same trend as observed in CCCC panel-2 with a slight variation in amplitude. Whereas for other cases the buckling mode shape changes drastically with modes moving towards clamped edge due to un-symmetric boundary conditions. Tables 17-18 depicts the effect of the thickness ratio on the buckling mode shape of a CCCC and CCFC panel-2 respectively. It can be noted from Tables 17-18 that thickness ratio has a significant effect on the buckling mode shape and its amplitude under all temperature cases.

   It can also be noted that the amplitude of the buckling modes decreases with the increase in thickness ratio. Tables 19-20 shows the influence of curvature ratio on the buckling mode shape on a CCCC and CCFC cylindrical panel-2 respectively. Where it can be seen that the buckling mode shape of CCCC and CCFC panel-2 is highly influenced by curvature ratio. As the curvature ratio increases buckling modes are moving towards the center of the CCCC panel-2 where the panel is less stiff. Similar behavior is observed under all temperature fields.

4.3.2 Free vibration dharacteristics

   A cylindrical panel-2 under non-uniform temperature is analyzed to study the effect of heat sink temperature on natural frequencies. Pre-stressed modal analysis has been carried out to determine free vibration frequency of a cylindrical panel-2 subjected to two different temperature fields

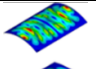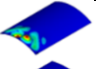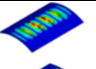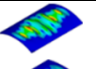Table 19 Effect of curvature ratio on buckling mode shape of CCCC panel-2
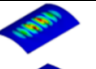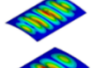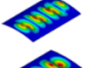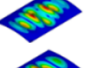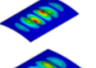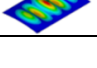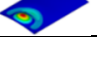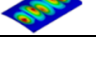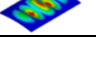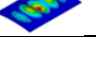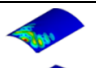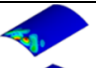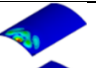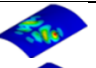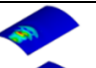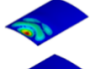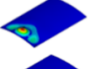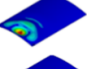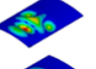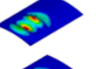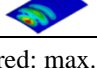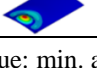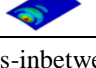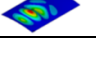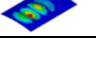
R/S	Case (i)	Case (ii)	Case (iii)	Case (iv)	Case (v)
1					
2					
3					

Table 20 Effect of curvature ratio on buckling mode shape of CCFC panel-2

R/S	Case (i)	Case (ii)	Case (iii)	Case (iv)	Case (v)
1					
2					
3					

Note: Dark-red: max.; dark-blue: min. and others-inbetween

Table 21 Effect of non-uniform thermal field on free vibration frequencies (Hz)

Mode	Ambient temperature	T_s/T_o (Case (v))						T_s/T_o (Case (iv))					
		0	0.2	0.4	0.6	0.8	1*	0	0.2	0.4	0.6	0.8	1*
1	205	168	177	185	192	199	205	186	190	194	198	201	205
2	315	295	301	305	309	313	315	297	302	306	309	313	315
3	384	340	349	358	361	376	384	368	371	375	378	381	384
4	490	463	469	475	480	485	490	485	486	487	488	489	490

under simply supported boundary conditions having free in-plane motion. Table 21 depicts the effect of non-uniform temperature variation on free vibration frequency in the absence of in-plane boundary constraints. A simply supported panel-2 with case (v) temperature field has a fundamental frequency of 168 Hz when the heat sink temperature is 0℃ above ambient temperature, which increases to 205 Hz when the heat sink temperature equals to peak temperature i.e., 100℃ above ambient temperature.

Similarly, for case(iv) it increases from 186 Hz to 205 Hz when panel temperature field changes from non-uniform to uniform. This is due to the fact that as the thermal stress reduces, the stiffness of panel increases and thus increases the frequency. It can also be seen that, case (v) temperature field has more influence on natural frequency compared to case (iv). Table 22 shows the effect of thermal load on free vibration frequency of CCCC and CCFC panel-2 under different temperature field. Results obtained in Table 22 clearly shows the significance of thermal load while determining the free vibration frequency. Because at higher temperature, panel becomes softer thus the stiffness of the panel decreases. Table 23 shows the variation of first five vibration modes of panel-2 under different temperature field. It is clear from the results that; the mode shapes are changing with the increase in temperature. The anti-nodal lines of the clamped cylindrical panel-2 are moving towards the maximum heat exposed portion of the panel. Behavior of free vibration modes of a panel-2 is similar to panel-1 under CCCC boundary conditions. It can

Table 22 Effect of thermal load on free vibration frequency (Hz)

Boundary condition	Mode	Ambient Temp.	Case (i)		Case (ii)		Case (iii)		Case (iv)		Case (v)	
			$0.5*T_{cr}$	$0.95*T_{cr}$	$0.5*T_{cr}$	$0.95*T_{cr}$	$0.5*T_{cr}$	$0.95*T_{cr}$	$0.5*T_{cr}$	$0.95*T_{cr}$	$0.5*T_{cr}$	$0.95*T_{cr}$
CCCC	1	1056	1009	724	986	791	966	782	986	796	968	862
	2	1328	1286	793	1268	877	1234	795	1260	804	1252	878
	3	1580	1445	953	1391	916	1392	844	1401	915	1364	879
	4	1614	1475	1235	1422	959	1431	959	1423	1168	1396	979
CCFC	1	788	770	720	756	718	753	678	758	725	750	708
	2	1232	1185	748	1165	749	1141	701	1155	786	1145	747
	3	1249	1221	788	1195	887	1198	931	1203	822	1199	789
	4	1387	1327	1092	1305	1062	1269	961	1287	1036	1289	1004

Table 23 Effect of thermal load on the free vibration mode shape of panel-2

Temp. Variation Cases	Temp.	CCFC					CCCC				
		Mode					Mode				
		1	2	3	4	5	1	2	3	4	5
	Ambient Temp.										
Case(i)	$0.5*T_{cr}$										
	$0.95*T_{cr}$										
Case(ii)	$0.5*T_{cr}$										
	$0.95*T_{cr}$										
Case(iii)	$0.5*T_{cr}$										
	$0.95*T_{cr}$										
Case(iv)	$0.5*T_{cr}$										
	$0.95*T_{cr}$										
Case(v)	$0.5*T_{cr}$										
	$0.95*T_{cr}$										

Note: Dark-red: max.; dark-blue: min. and others-inbetween

be noticed from Table 23 that the buckling mode shape at 50% of buckling load is similar for all temperature cases, whereas at 95% of buckling load, it is found that anti-nodal lines are moving towards the maximum heat source as panel is found to be softer at maximum heat source. To know the effect of boundary conditions on the free vibration modes, a cylindrical panel-2 with CCFC boundary condition has also been considered. Result of the analysis shows that; the mode shapes

are changing with the increase in temperature. But there is not much significant effect can be observed in the panel-2 as compared to panel-1 under CCFC boundary conditions. This is due to the fact, as the aspect ratio (*L/S*) of the panel increases influence of thermal load on the free vibration mode shape is not so significant.

5. Conclusions

In this paper an investigation has been done on the cylindrical panels subjected to various non-uniform temperature field in order to study the critical buckling and the free vibration behavior of the panel. A numerical approach is used for the same using finite element method based software ANSYS. Materials properties consider for the analysis are assumed to be temperature independent. The results show that the buckling and free vibration behavior of cylindrical panels under thermal load is complex and greatly influenced by the temperature field, elevated temperature, geometric parameter and in-plane boundary conditions. Therefore, the following conclusion can be drawn:
  • "Magnification factor of the first kind, (η)" was established to relate critical buckling temperature obtained under uniform temperature with non-uniform temperature field.
  • "Magnification factor of the second kind, (ζ)" was established to study the effect of heat sink temperature on the buckling behavior of cylindrical panel under simply supported condition with free in-plane motion.
  • The buckling strength of the panel under thermal load is significantly influenced by non-uniform temperature variation field as it has the tendency of producing different kind of thermal stress in panel.
  • Fundamental buckling mode and free vibration mode shapes are significantly influenced by the nature of temperature variation along with the geometric variation and structural boundary conditions.
  • The buckling strength of the panel-2 is higher than the panel-1, whereas the free vibration frequency of panel-2 is lesser than the panel-1when subjected to non-uniform temperature distribution.
  • Influence of non-uniform temperature variation on fundamental buckling mode shapes and free vibration mode shapes are more significant for panel-2 compared to panel-1.

References

Al-Khaleefi, A.M. (2004), "Thermal buckling of clamped cylindrical panels based on first-order shear deformation theory", *Int. J. Struct. Stab. Dyn.*, **4**(3), 313-336.
Au, F. and Cheung, Y. (1996), "Free vibration and stability analysis of shells by the isoparametric spline finite strip method", *Thin Wall. Struct.*, **24**(1), 53 - 82.
Averill, R.C. and Reddy, J.N. (1993), "Thermomechanical postbuckling analysis of laminated composite shells", *Structural Dynamics and Materials Conference*, 351-360.
Baruta, A., Madencia, E. and Tesslerb, A. (2000), "Nonlinear thermoelastic analysis of composite panels under non-uniform temperature distribution", *Int. J. Solid. Struct.*, **37**, 3681-3713.
Buchanan, G.R. and Rich, B.S. (2002), "Effect of boundary conditions on free vibration of thick isotropic spherical shells", *J. Vib. Control*, **8**(3), 389-403.
Chen, L.W. and Chen, L.Y. (1987), "Thermal buckling of laminated cylindrical plates", *Compos. Struct.*, **8**(3), 189-205.

Chen, W., Lin, P. and Chen, L. (1991), "Thermal buckling behavior of thick composite laminated plates under non-uniform temperature distribution", *Comput. Struct.*, **41**(4), 637-645.

Ganapathi, M., Patel, B. and Pawargi, D. (2002), "Dynamic analysis of laminated cross-ply composite non-circular thick cylindrical shells using higher-order theory", *Int. J. Solid. Struct.*, **39**(24), 5945-5962.

Ganesan, N. and Pradeep, V. (2005), "Buckling and vibration of circular cylindrical shells containing hot liquid", *J. Sound Vib.*, **287**(4-5), 845-863.

Jeng-Shian, C. and Wei-Chong, C. (1991), "Thermal buckling analysis of anti- symmetric laminated cylindrical shell panels", *Int. J. Solid. Struct.*, **27**(10), 1295-1309.

Jeon, B.H., Kang, H.W. and Lee, Y.S. (2010), "Free vibration characteristics of thermally loaded cylindrical shell", *Mater. Complex Behav.*, **3**, 139-148.

Jeyaraj, P. (2013), "Buckling and free vibration behavior of an isotropic plate under non-uniform thermal load", *Int. J. Struct. Stab. Dyn.*, **12**(6), 1-16.

Kdoli, R. and Ganesan, N. (2006), "Buckling and free vibration analysis of functionally graded cylindrical shells subjected to a temperature-specified boundary condition", *J. Sound Vib.*, **289**(3), 450-480.

Ko, W.I. (2004), "Thermal buckling analysis of rectangular panels subjected to humped temperature profile heating", *Struct. Mech.*, **57**, 1-34.

Kurpa, L., Shmatko, T. and Timchenko, G. (2010), "Free vibration analysis of laminated shallow shells with complex shape using the R-functions method", *Compos. Struct.*, **93**(1), 225-233.

Narita, Y., Ohta, Y. and Saito, M. (1993), "Finite element study for natural frequencies of cross-ply laminated cylindrical shells", *Compos. Struct.*, **26**(1-2), 55-62.

Reddy, J. and Liu, C. (1985), "A higher-order shear deformation theory of laminated elastic shells", *Int. J. Eng. Sci.*, **23**(3), 319-330.

Ross, B., Hoff, N. and Horton, W. (1966), "The buckling behavior of uniformly heated thin circular cylindrical shells", *Exper. Mech.*, **6**(11), 529-537.

Sk, L. and Sinha, P.K. (2005), "Improved finite element analysis of multilayered, doubly curved composite shells", *J. Reinf. Plast. Compos.*, **24**(4), 385-404.

Zhao, X., Ng, T.Y. and Liew, K. (2004), "Free vibration of two-side simply- supported laminated cylindrical panels via the mesh-free kp-ritz method", *Int. J. Mech. Sci.*, **46**(1), 123-142.

CC